Solid State Sciences 12 (2010) 660–664

Contents lists available at ScienceDirect

Solid State Sciences

journal homepage: www.elsevier.com/locate/ssscie

Magnetic and crystal structures of $BiCrO_3$

C. Darie [a,*], C. Goujon [a], M. Bacia [a], H. Klein [a], P. Toulemonde [a], P. Bordet [a], E. Suard [b]

[a] Institut Néel/CNRS/UJF_25, rue des Martyrs F, BP166 38042 Grenoble cedex, France
[b] Institut Laue-Langevin, BP156, 38042 Grenoble cedex 9, France

ARTICLE INFO

Article history:
Received 2 July 2008
Received in revised form
4 December 2008
Accepted 7 December 2008
Available online 24 December 2008

Keywords:
$BiCrO_3$
Magnetic structure
Powder neutron diffraction

ABSTRACT

Polycrystalline samples of $BiCrO_3$ were synthesized by high pressure–high temperature solid state reaction in a Conac anvil-type apparatus at 2 GPa and 805 °C. Neutron powder diffractograms were collected on the D20 and D2B instruments of the ILL-Grenoble between 2 K and 470 K. Magnetic susceptibility measurements show the onset of magnetic order at 110 K followed by a large increase below 80 K. The neutron diffraction data indicate the appearance of G-type antiferromagnetic order at the 114 K transition temperature, with all spins aligned along one of the unit cell axes and antiparallel spins on different Cr sites. This is followed by a progressive spin reorientation between 80 K and 60 K.

1. Introduction

In the last few years, the study of multiferroic compounds has undergone a large development. This is largely due to the discovery of magneto-electric coupling and appearance of electric polarization at a low temperature magnetic phase transition, in materials which are not ferroelectric in their non-magnetically ordered state [1]. Despite their considerable interest for the fundamental understanding of multiferroic properties, these materials might be of little applicability because of the weakness of their magnetic/electric polarizations and of the low temperatures at which these properties are observed. From this point of view, more "classical" multiferroics, i.e. ferroelectric compounds which order magnetically, are now subject of a renewed interest since they remained largely unexplored until recently.

Among these materials, the $BiMO_3$ perovskites (M = magnetic 3d metal cation, Mn, Fe, Cr) are the most promising for applications. $BiFeO_3$ is ferroelectric ($T_C \approx 1100$ K), antiferromagnetic ($T_N \approx 643$ K), and exhibits weak magnetism at room temperature. It can be prepared as thin films and large crystals [2]. The situation is more ambiguous for $BiMnO_3$, which can only be synthesized at high pressure. $BiMnO_3$ undergoes a phase transition at 760 K and becomes ferromagnetic below 105 K. Depending on the authors, the space group of the low temperature phase could be $C2$ or $C2/c$, as recently reported from convergent-beam electron diffraction or neutron powder diffraction [3–5]. The $C2/c$ space group is centrosymmetric and thus prevents the possibility of ferroelectricity in $BiMnO_3$. More recently, Kodama et al. [6] performed a PDF analysis of neutron powder diffraction data and proposed as real symmetry $P2$ or $P2_1$ on the local scale, with the formation of domains of size >100 Å.

$BiCrO_3$ is the least investigated compound of the series. Theoretical studies [7,8] based on first characterizations [9,10] predicted a multiferroic behaviour. $BiCrO_3$ was reported to have the same structure as $BiMnO_3$. Studies on thin film showed antiferroelectric properties consistent with a centrosymmetric crystal structure [11]. Magnetic studies available up to now concluded the appearance of an antiferromagnetic transition with a weak spontaneous moment below 114 K. The weak spontaneous moment increases rapidly below 95 K, with a difference between the zero-field-cooled and field-cooled magnetization curves below 75 K. Recently [12] an extensive study on magnetic properties on a single-phased powder $BiCrO_3$ showed four anomalies of magnetic origin near 40, 75, 109 and 111 K. The long-range antiferromagnetic order with weak ferromagnetism is found to occur at $T_N = 109$ K. The ac susceptibilities showed that the transition near T_N is a two-step transition.

Using TEM, X-ray and neutron powder diffraction we showed that $BiCrO_3$ has a structure very close to that of $BiMnO_3$, but is twinned with domain sizes of a few nanometers [13], which prevents precise structural analysis by classical diffraction tools. We have now undertaken the synthesis of a large quantity of polycrystalline $BiCrO_3$ under HP–HT (high temperature–high pressure)

* Corresponding author. Tel.: +33 04 76 88 79 40; fax: +33 04 76 88 10 38.
E-mail address: celine.darie@grenoble.cnrs.fr (C. Darie).

1293-2558/$ – see front matter © 2008 Elsevier Masson SAS. All rights reserved.
doi:10.1016/j.solidstatesciences.2008.12.004

to perform neutron diffraction. This technique was applied in three directions: (a) the phase transitions at HT and the structure determination of the orthorhombic HT phase, (b) the determination of the structure at room temperature (monoclinic form), (c) the determination of the magnetic structure at low temperature.

2. Experimental

Polycrystalline samples of $BiCrO_3$ were synthesized by solid state reaction under HP–HT. As starting materials a mixture of powders of Bi_2O_3 (Aldrich, 99.9%) and Cr_2O_3 (Prolabo, 99%) in the stoechiometric proportions was packed into a gold capsule ($d = 6$ mm, $h = 6$ mm), and heated in a Conac 28 anvil-type apparatus. The optimized synthesis conditions were 2 GPa and 805 °C [13]. Eight syntheses were performed to obtain about 3 g of powder. Each batch was checked by X-ray diffraction on a D5000R diffractometer operating in reflection mode and equipped with CoKα radiation ($l = 1.7890$ Å).

Neutron powder diffraction (NPD) data were collected on the D20 and D2B instruments of the Institut Laue Langevin – Grenoble. For the D20 experiment, a 2.41 Å wavelength from the (002) reflection of a HOPG monochromator was used. The sample was put inside a cylindrical vanadium can itself placed in an orange cryostat. The sample was first cooled down to 2 K then heated up to 500 K and brought back to room temperature while powder neutron diffraction data were recorded "on the fly" about every minute. The D2B measurements were carried out at selected temperatures (2 K, 90 K, 130 K, 300 K, 470 K) using a pulse tube cryostat with a 1.59 Å wavelength from a Ge(335) monochromator. In order to optimize spatial resolution, only the central part in the axial direction of the 2D detector data was integrated. All refinements were done using the WinplotR/Fullprof software [14].

3. Results and discussion

3.1. Crystal structure

On heating above room temperature, a phase transition is observed at about 430 K with a clear symmetry change. The high temperature phase structure was refined from D2B data at 470 K. The sample contained a small amount of impurities identified as bismuthite ($Bi_2O_2CO_3$) and cubic Bi_2O_3; both these phases were taken into account in the refinement, which gave a proportion of impurities representing 3% of the sample weight. The structure is of the orthoferrite type, with unit cell parameters $a = 5.5427(1)$ Å, $b = 7.7524(2)$ Å, $c = 5.4255(1)$ Å and *Pnma* space group. Refined structural parameters and relevant interatomic distances and angles are given in Table 1; the quality of the refinement can also be assessed from Fig. 1. The CrO_6 octahedra are almost regular, with cation to oxygen distances slightly smaller than 2 Å and O–Cr–O angles between 89° and 91.1°. On the other hand, the Bi coordination polyhedra are strongly distorted, with Bi–O distances ranging from 2.33 Å to 3.35 Å. This is probably due to the presence of the stereo-active electron lone pair.

In order to investigate the issue of the existence of an inversion centre in $BiCrO_3$, the NPD data collected on D2B at room temperature were refined with the *C*2/*c* and *C*2 space groups.

The monoclinic unit cell is related to the perovskite cubic axes by the matrix:

$$\begin{pmatrix} \vec{a}_m \\ \vec{b}_m \\ \vec{c}_m \end{pmatrix} = \begin{pmatrix} \bar{1} & \bar{2} & 1 \\ 1 & 0 & 1 \\ \bar{1} & 2 & 1 \end{pmatrix} \begin{pmatrix} \vec{a}_p \\ \vec{b}_p \\ \vec{c}_p \end{pmatrix}$$

Given the presence of strong correlations which prevented the convergence of the *C*2 symmetry refinement, the Biso parameters of each atom type were constrained to be equal. This was unnecessary for space group *C*2/*c*. The agreement factors are similar for both refinements, as can also be visualized from inspection of the difference plots (Fig. 2). The results of the *C*2/*c* refinement at 300 K, 90 K and 2 K together with interaction distances at *RT* are given in Table 2. No reflection of the type (*h*0*l*) with *l* odd which would break the extinction condition for the *c* glide plane is found to yield a detectable intensity. These observations lead us to conclude that the symmetry of $BiCrO_3$ is *C*2/*c*, at least as observed by standard crystallographic methods.

Contrary to the high temperature phase case, noticeable discrepancies are observed in the Rietveld difference plots with room temperature data. Strong anisotropic peak broadening associated with the presence of diffuse scattering between strong Bragg reflections is observed, which could not be properly taken into account despite many efforts. These features can be attributed to the existence of twin domains with sizes of the order of 10 nm revealed by transmission electron microscopy. These domains are created on cooling from the more symmetrical, high-temperature phase. The presence of such small domains leads to a certain inaccuracy in the modelling of the diffraction profile, and consequently of the refined parameters. Since these domains persist at

Table 1
Structural parameters and cation–anion distances (Å) for $BiCrO_3$ at 470 K obtained by Rietveld refinement of D2B NPD data.

Atom	*X*	*Y*	*Z*	Biso (Å^2)
Bi1	0.0432(4)	1/4	−0.0051(6)	1.31(5)
Cr1	1/2	1/2	0	0.67(8)
O1	0.4793(6)	1/4	0.0811(6)	0.97(6)
O2	0.2948 (5)	0.0390(3)	0.7015(5)	1.22(5)
Bi1-O1: 3.160(4)			Bi1-O1: 2.462(4)	
Bi1-O1: 3.145(5)			Bi1-O1: 2.328(5)	
Bi1-O2 (x2): 2.675(3)			Bi1-O2 (x2): 2.389(3)	
Bi1-O2 (x2): 3.353(3)			Bi1-O2 (x2): 2.661(3)	
Average: *2.77*				
Cr1-O1 (x2): 1.9906(7)			Cr1-O2 (x2): 1.989(3)	
Cr1-O2 (x2): 2.002(3)				
Average: *1.99*				

Space group *Pnma* (*n*°62) ; $a = 5.5427(1)$ Å, $b = 7.7524(2)$ Å, $c = 5.4255(1)$ Å ; Rwp: 20.6, Chi2: 2.41.

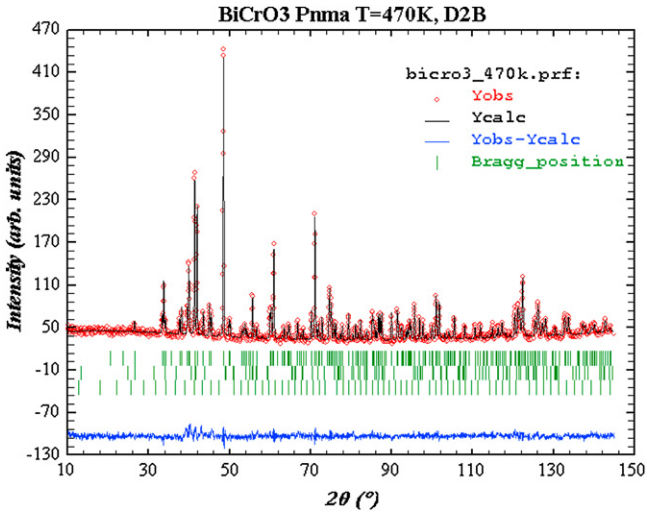

Fig. 1. Rietveld plot for $BiCrO_3$ at 470 K from D2B neutron powder diffraction data.

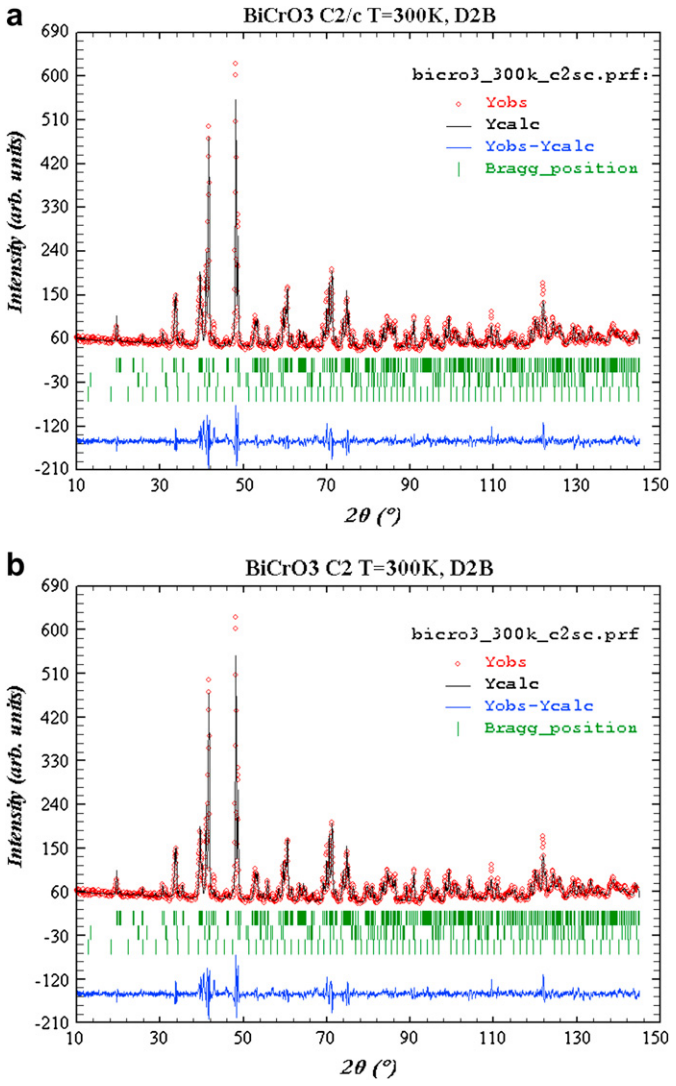

Fig. 2. Rietveld plot for $BiCrO_3$ at 300 K from D2B neutron powder diffraction data. Refinement with space group (a) *C*2/*c*, (b) *C*2.

low temperature, this detrimental effect will also exist for the analysis of the magnetic structure using NPD.

In order to check whether these discrepancies in the Rietveld refinements could due to the presence of another phase, high resolution synchrotron diffraction data were collected on the ID31 beam line of the ESRF ($\lambda = 0.398$ Å). As an illustrative example, Fig. 3 shows the part of the diffractogram comprising the (2 0 2), (−1 1 3), (0 2 0) and (−3 1 1) Bragg reflections around 8.3°. The calculated profile is from a tentative LeBail refinement in *C*2 symmetry. Quite clearly, the discrepancies between the observed and calculated profiles and particularly the presence of continuous diffuse scattering between 8.27° and 8.35° cannot be attributed to the presence of a single additional phase. These effects are more probably due to local disorder related to the presence of nano-domains, as stated above and evidenced by transmission electron microcopy. As a paradox, due to a poorer instrumental resolution which can smooth out the sample broadening and diffuse scattering effects, Rietveld refinements of the NPD data can yield better agreements and lead to acceptable results.

To conclude, our present results indicate in agreement with Ref. [5] a centrosymmetric structure preventing the possibility of ferroelectricity for $BiCrO_3$. PDF analysis of synchrotron X-ray powder diffraction data is under way to investigate the existence of local structural distortions and/or the effects of twin domains on the physical properties.

Table 2
Structural parameters for $BiCrO_3$ at 300 K, 90 K and 2 K[a] obtained by Rietveld refinement of D2B neutron powder diffraction data.

Atom	*X*	*Y*	*Z*	Biso (Å^2)
Bi1	0.1331(4)	0.2166(6)	0.1313(4)	0.74(7)
	0.1337(5)	0.2152(8)	0.1309(5)	0.44(8)
	0.1334(6)	0.2158(0)	0.1313(6)	0.46(9)
Cr1	1/4	1/4	1/2	0.6(2)
	1/4	1/4	1/2	0.7(2)
	1/4	1/4	1/2	0.6(3)
Cr2	0	0.237(2)	3/4	0.8(2)
	0	0.237 (2)	3/4	0.8(2)
	0	0.235(3)	3/4	0.9(3)
O1	0.0860(5)	0.204(1)	0.5869(5)	0.9 (1)
	0.0872(7)	0.203(1)	0.5874(7)	0.7(1)
	0.0873(8)	0.202(2)	0.5870(8)	0.8(1)
O2	0.1552(6)	0.523(1)	0.3643(6)	1.2(1)
	0.1554(8)	0.521(1)	0.3644(8)	1.1(1)
	0.1557(0)	0.523(2)	0.3649(0)	1.1(2)
O3	0.3582(6)	0.526(1)	0.1590(5)	0.5(8)
	0.3561(7)	0.522(1)	0.1588(7)	0.2(1)
	0.3575(9)	0.522(2)	0.1596(9)	0.5(1)
Bi1-O1: 3.218(7)		Bi1-O2: 2.748(7)		Bi1-O3: 2.669(7)
Bi1-O1: 3.160(5)		Bi1-O2: 3.216(7)		Bi1-O3: 2.895(7)
Bi1-O1: 2.433(5)		Bi1-O2: 2.997(7)		Bi1-O3: 2.245(6)
Bi1-O1: 2.360(7)		Bi1-O2: 2.258(7)		Bi1-O3: 3.108(7)
Cr1-O1 (x2): 1.998(5)		Cr1-O2 (x2): 1.997(6)		Cr1-O3 (x2): 1.973(5)
Cr2-O1 (x2): 1.988(5)		Cr2-O2 (x2): 2.019(9)		Cr2-O3 (x2): 1.971(9)

Space group *C*2/*c* (N°15) and cation–anion distances (Å) for $BiCrO_3$ at 300 K.
[a] The first line of each site (*x*,*y*,*z*,Biso) is for 300 K, the second line for 90 K and the third line is for 2 K. 300 K: unit cell $a = 9.4681(2)$ (Å), $b = 5.4822(1)$ (Å), $c = 9.5865(2)$ (Å), $\beta = 108.574(1)$ Rwp: 22.1, Chi2: 4.76, RBragg: 7.47. 90 K: unit cell $a = 9.4540(2)$ (Å), $b = 5.4752$ (1) (Å), $c = 9.5771(2)$ (Å), $\beta = 108.55(2)$ Rwp: 28.3, Chi2: 3.14, RBragg: 10.1. 2 K unit cell $a = 9.45191(22)$ (Å), $b = 5.4741(1)$ (Å), $c = 9.5767(2)$ (Å), $\beta = 108.55(2)$ (1) Rwp: 34.5, Chi2: 2.10, RBragg: 11.7.

3.2. Magnetic structure

The D20 NPD data at low temperature show the appearance of magnetic contributions into the nuclear Bragg peaks at 114 K on cooling. This is followed by a strong increase in intensity starting at 80 K (Fig. 4). No hysteretic behaviour could be observed on

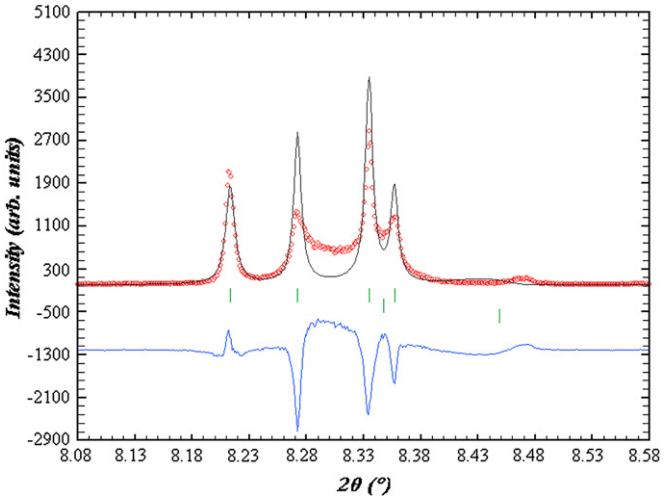

Fig. 3. Part of the synchrotron XRD diffractogram showing the (2 0 2), (−1 1 3), (0 2 0) and (−3 1 1) Bragg reflections around 8.3° (ESRF ID31). The calculated profile is from a tentative LeBail refinement in *C*2 symmetry.

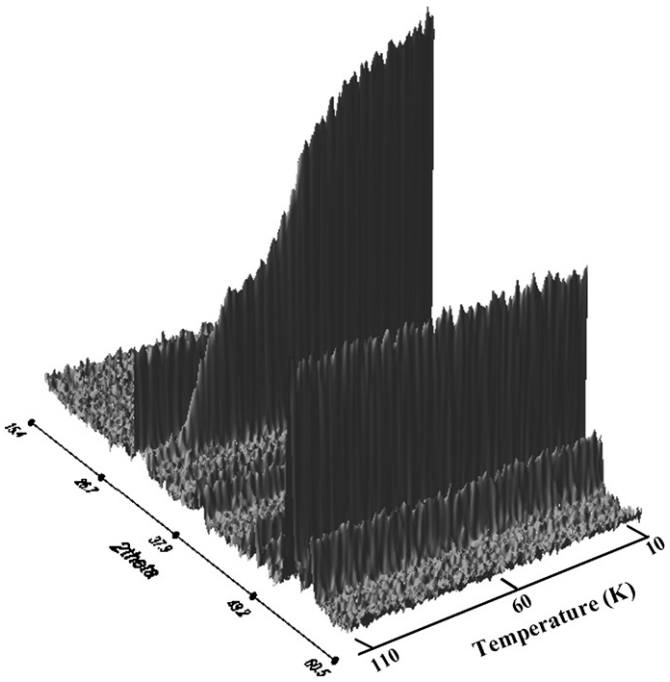

Fig. 4. Part of the neutron diffractogram of $BiCrO_3$, on cooling between 110 K and 10 K showing the increase of the intensity of the magnetic peak.

heating. On Fig. 5 are reported the structural parameters (a,b,c and β) as a function of the temperature. These indicate clearly that the structure is not modified under temperature. All magnetic peaks can be indexed with the C-centred nuclear cell, which contains 4 crystallographically independent Cr cations. Refinements of the nuclear and magnetic structures were carried out at 90 K from the D2B NPD data. The best solution (Chi2: 3.16, RBragg: 10.1, RMag: 13.5) was obtained for a magnetic structure consisting in a collinear antiferromagnetic arrangement of equal Cr^{3+} cation moments along the b axis of the monoclinic cell (i.e. the (101) face diagonal of the perovskite cell). The moments of all the first neighbours of each Cr^{3+} cation moment are aligned antiparallel to

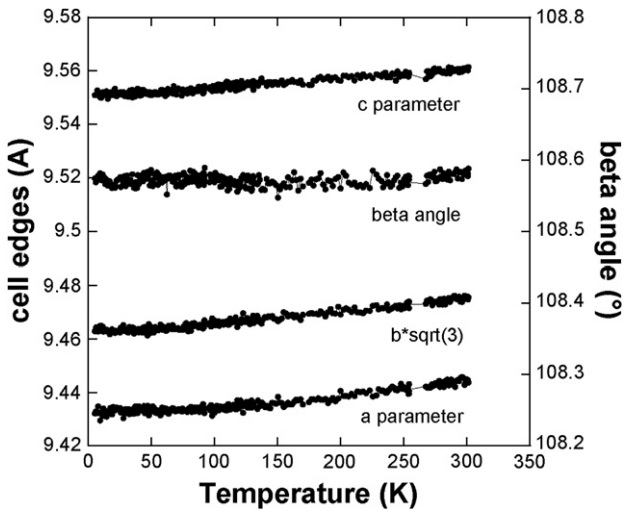

Fig. 5. Structural parameters (a,b,c and β) from D20 neutron powder diffraction under temperature.

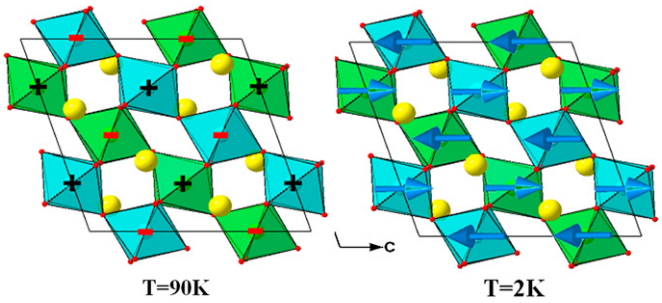

Fig. 6. Magnetic structure of $BiCrO_3$, projected along the b axis direction at (a) 90 K (spin up (+), spin down (−)) and (b) 2 K (after reorientation of the spin).

it (Fig. 6a). The refined modulus of the Cr^{3+} moment was 2.04(8) μB at 90 K.

The structure refined at 2 K (Chi2: 2.09, RBragg: 11.8, RMag: 12.2) indicates a reorientation of the moment directions while conserving the global collinear antiferromagnetic arrangement of the 90 K magnetic structure. The moments have rotated in the (b,c) plane to form $a \approx 50°$ angle with the b axis direction (Fig. 6b). This spin reorientation process is best visualized in Fig. 7, where the common modulus of the Cr^{3+} moments and their angle theta with respect to the b axis directions are reported as function of temperature. These results were obtained by sequential refinement of the D20 NPD data using the magnetic structure models obtained from the D2B data. It is clear that the increase of the intensity of magnetic contributions observed below 80 K has to be attributed to the beginning of the spin reorientation process, which takes places in a temperature range between 80 K and ≈60 K. It is also worth noting that the moduli of the Cr^{3+} moments gradually increase on cooling between the upset of magnetic order at 114 K to saturate around 2.6 μB at the lowest investigated temperatures, without perturbation from the spin reorientation process. On the same figure are superimposed the field-cooled and zero-field-cooled susceptibilities vs T magnetization curves. Clearly, the first step in the magnetization curve at ≈110 K is due to the appearance of magnetic order, while the large magnetization increase starting

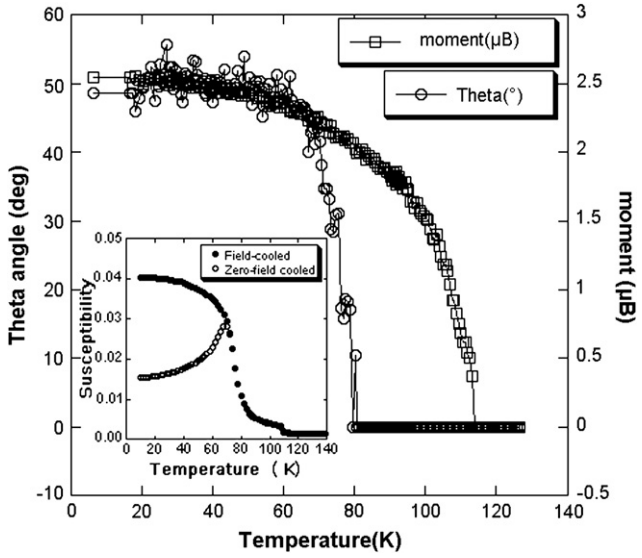

Fig. 7. Representation of the common modulus of the Cr^{3+} moments (□), their angle with respect to the b axis directions (○) vs temperature and inset: field-cooled and zero-field-cooled susceptibilities' curves in $BiCrO_3$.

around 80 K coincides with the spin reorientation. The presence of a weak ferromagnetic contribution at low temperature was reported [10,12]. This is not permitted by our refined magnetic structure model, since all moments were constrained to have the same moduli and directions at all temperatures. Attempts to release these constraints in various ways always lead to unstable refinements. This can be attributed to the weakness of the expected ferromagnetic resultant and to the effect of twin domains, which degrades the profile refinement quality and thus limits the possibility to detect such a small ferromagnetic contribution. Note that in a recent study, Belik et al. [15] reported a similar G-type antiferromagnetic structure, with similar values for magnetic moment (2.55 μB at 7 K) but were also unable to refine the spin canting of magnetic moments occurring due to the spin reorientation process evidenced here.

4. Conclusion

The use of several powder neutron diffractometers of low and high temperatures allowed us to bring new accurate data on the crystal and magnetic structures of the "less studied" $BiCrO_3$. At high temperature the orthorhombic form with *Pnma* space group and unit cell parameters $a = 5.5427(1)$ Å, $b = 7.7524(2)$ Å, $c = 5.4255(1)$ Å is confirmed. The temperature of transition on heating is 430 K. At room temperature, we show that the quality of the structure determination is limited by twinning with 10 nm domains. We conclude that the room-temperature structure is monoclinic with $C2/c$ space group, $a = 9.4681(2)$ Å, $b = 5.4822(1)$ Å, $c = 9.5865(2)$ Å, $\beta = 108.574(1)^\circ$. The magnetic structure is a G-type antiferromagnetic order with moments aligned along b axis which appears below 114 K. A progressive spin reorientation takes place between 80 K and 60 K which corresponds to the large magnetization increase. No evidence of the weak ferromagnetic contribution could be refined with these data.

Acknowledgement

The authors wish to thank Andy Fitch and the staff at the ID31 ESRF Beamline for their experimental help.

References

[1] N. Hur, S. Park, P.A. Sharma, J.S. Ahn, S. Guha, S.W. Cheong, Nature 429 (2004) 392.
[2] J. Wang, J.B. Neaton, H. Zheng, V. Nagarajan, S.B. Ogale, B. Liu, D. Viehland, V. Vaithyanathan, D.G. Scholm, U.V. Waghmare, N.A. Spaldin, K.M. Rabe, M. Wuttig, R. Ramesh, Science 299 (2003) 1719.
[3] A.A. Belik, S. Iikubo, T. Yokosawa, K. Kodama, N. Igawa, Azuma M. Shamoto, M. Takano, K. Kimoto, Y. Matsui, E. Takayama-Muromachi, J. Am. Chem. Soc. 129 (2007) 971.
[4] E. Montanari, G. Calestani, L. Righi, E. Gilioli, F. Bolzoni, K.S. Knight, P.G. Raedaelli, Phys. Rev. B 75 (2007) 220101.
[5] T. Yokosama, A.A. Belik, T. Asaka, K. Kimoto, E. Takayama-Muromachi, Y. Matsui, Phys. Rev. B 77 (2008) 024111.
[6] K. Kodoma, S. Iikubo, S. Shamoto, A.A. Belik, E. Takayama-Muromachi, J. Phys. Soc. Jpn. 76 (12) (2007) 124605.
[7] N.A. Hill, P. Baettig, C. Daul, J. Phys. Chem. B 106 (2002) 3383.
[8] P. Baettig, C. Ederer, N.A. Spaldin, Phys. Rev. B 72 (2005) 214105.
[9] F. Sugawara, S. Iiida, Y. Syono, S. Akimoto, J. Phys. Soc. Jpn. 25 (1968) 1553.
[10] S. Niitaka, M. Azuma, M. Takano, E. Nishibori, M. Takata, M. Sakata, Solid State Ionics 172 (2004) 557.
[11] D.H. Kim, H.N. Lee, M. Varela, H.M. Christen, Appl. Phys. Lett. 89 (2006) 162904.
[12] A.A. Belik, N. Tsujii, H. Suzuki, E. Takayama-Muromachi, Inorg. Chem. 46 (2007) 8746.
[13] C. Goujon, C. Darie, M. Bacia, H. Klein, L. Ortega, P. Bordet, J. Phys. Conf. Ser. 121 (2008) 022009.
[14] J. Rodriguez-Carvajal, Physica B 192 (1993) 55.
[15] A.A. Belik, S. Iikubo, K. Kodama, N. Igawa, S. Shamoto, E. Takayama-Muromachi, Chem. Mater. 20 (2008) 3765.